The Journal of Chulabhorn Royal Academy
eISSN : 2697-5203 (Online)

Research article

Pathology of Acute Coronary Syndrome, Assessed Using Optical Coherence Tomography

Viroj Muangsillapasart, Plasat Laothavorn, Chompol Piamsomboon, Sopon Sanguanwong, Tanyarat Aramsaruwong, Supawat Ratanapo, Nakarin Sansanayudh*

Cardiovascular Division, Department of Internal Medicine, Phramongkutklao hospital

*Corresponding Author e-mail: dr_nakarin@hotmail.com

Abstract

Objectives: We aimed to characterize the pathology of patients with acute coronary syndrome (ACS) using optical coherence tomography (OCT).
Background: OCT is a new, high-resolution intravascular imaging modality that is useful for the assessment of the morphology of ACS lesions.
Methods: We studied 22 patients with ACS using OCT imaging. The pathological features of the disease were classified as plaque rupture, plaque erosion, and calcified nodule.
Results: The incidences of plaque rupture, plaque erosion, and calcified nodule were 73%, 9%, and 9%, respectively. Participants with plaque rupture tended to be younger than those with the other types of lesions (65.7 ± 9.4, 72.0 ± 9.9, and 80.0 ± 8.5 years, respectively; p=0.13). Fibrous plaque tended to be more prevalent than plaque erosion (75%, 100%, and 0%, respectively; p=0.15). The serum creatinine concentration of participants with calcified nodule was higher than that of participants with plaque rupture (1.2 ± 0 *vs*. 1.0 ± 0.2; p=0.049). The mean minimum luminal diameter (MLD) was highest in participants with calcified nodule and was significantly higher than in participants with plaque rupture (1.5 ± 0.5 *vs*. 1.0 ± 0.2; p=0.047).
Conclusions: Plaque rupture was the most common lesion, being present in 73% of the patients with ACS, and plaque erosion tended to be associated with the lowest mean luminal area of the three types of lesions. In addition, calcified nodules were common in older patients and were associated with a higher creatinine concentration and MLD than plaque rupture.

Keywords: Plaque rupture, Plaque erosion, Calcified nodule, Optical coherence tomography, Acute coronary syndrome

© Chulabhorn Royal Academy. Terms and conditions of Creative Commons Attribution 4.0 International (CC BY NC ND 4.0) apply

Introduction

Acute coronary syndrome (ACS) is one of the commonest causes of sudden cardiac death. In most instances, ACS is thought to be the result of sudden coronary stenosis, secondary to thrombosis. Luminal thrombosis can occur as a result of three pathological changes in particular: plaque rupture (PR), plaque erosion (PE), and calcified nodule (CN). The incidence of thrombus in patients who suddenly die because of ACS is ~60%, and the underlying etiologies have been shown to be PR in 55%–60% of cases, PE in 30%–35%, and CN in 2%–7% [(1)]. In addition, Naghavi et al. found that plaque rupture is the most common lesion at autopsy in patients who experience sudden cardiac death [(2)].

Optical coherence tomography (OCT) is an intravascular imaging technique that is based on the reflection of near-infrared light to create images, and this provides a high axial resolution of up to 10 µm and lateral resolution of 20 µm. The tissue penetration is limited to a depth of 2 mm, but this varies significantly, according to the tissue being imaged. At present, the resolution achievable using OCT is superior to that of other intravascular imaging techniques [(3)]. For example, it is up to 10 times higher than that of intravascular ultrasonography (IVUS), such that it can provide clear detail of the three layers of the vascular wall. Many previous studies have shown that OCT can be used to visualize the microstructure of atherosclerotic plaques, including the thin fibrous cap, lipid core, and intracoronary thrombus, which are believed to be responsible for plaque vulnerability [(4–6)]. OCT images of atherosclerotic plaque provide more detail of the microstructure than IVUS [(5)].

In the present study, we aimed to evaluate the pathological characteristics of PR, PE, and CN lesions in patients with ACS (including ST segment elevation myocardial infarction [STEMI] and non-ST segment elevation acute coronary syndrome [NSTACS]) using OCT.

Methods

Study sample

We recruited 22 patients with ACS who underwent OCT imaging of their culprit lesions. The exclusion criteria were failure in the advance of the OCT catheter across the culprit lesion; contamination with blood, which results in poor image quality; severe calcification, necessitating rotational atherectomy (Rotablator; Boston Scientific, Marlborough, MA, USA), and chronic kidney disease (CKD) stages IV and V.

The participants had either STEMI or NSTE-ACS. ST segment elevation myocardial infarction (MI) was defined using continuous chest pain that lasted >20 min; ST segment elevation on more than two contiguous leads of ≥ 2.5 mm in men < 40 years, ≥ 2 mm in men ≥ 40 years, or ≥ 1.5 mm in women on lead V2/V3, and/or ≥ 1 mm on other leads, or new left bundle-branch block. NSTE-ACS included non-ST segment elevation myocardial infarction (NSTEMI) and unstable angina pectoris. NSTEMI was defined using ischemic symptoms in the absence of ST segment elevation on electrocardiography, with high circulating cardiac enzyme activities. Unstable angina pectoris was defined as new-onset chest discomfort on exertion or at rest, with normal concentrations of cardiac markers. The study was approved by the Phramongkutklao Medical College Ethics Committee and all the participants provided their written informed consent.

OCT image acquisition

OCT imaging of culprit lesions was conducted using the frequency domain Optis system and a Dragonfly Optis Imaging Catheter or the OFDI system and an OFDI catheter. The culprit lesion was identified using coronary angiography, electrocardiography, and transthoracic echo-cardiography. In participants with TIMI flow ≤ 2, aspiration thrombectomy or pre-dilatation with a balloon of diameter less than that of the vessel was performed. A 2.7-F OCT imaging catheter was carefully advanced distal to the culprit lesion, then automatic or manual pullback was performed at 40 mm/sec for 7.5 cm, while contrast media was gradually added to replace the blood removed.

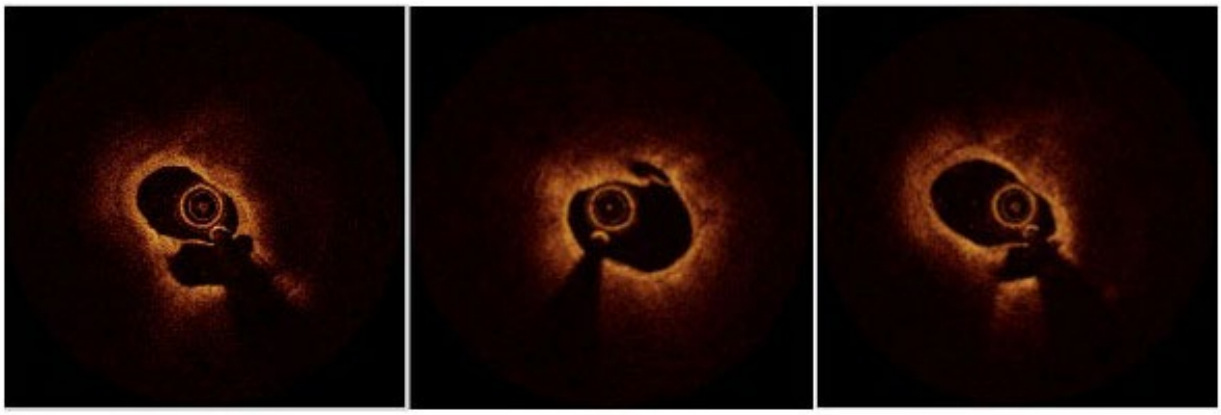

Figure 1. OCT images showed plaque rupture was identified by a presence of fibrous cap discontinuity and a caviry formation of the plaque

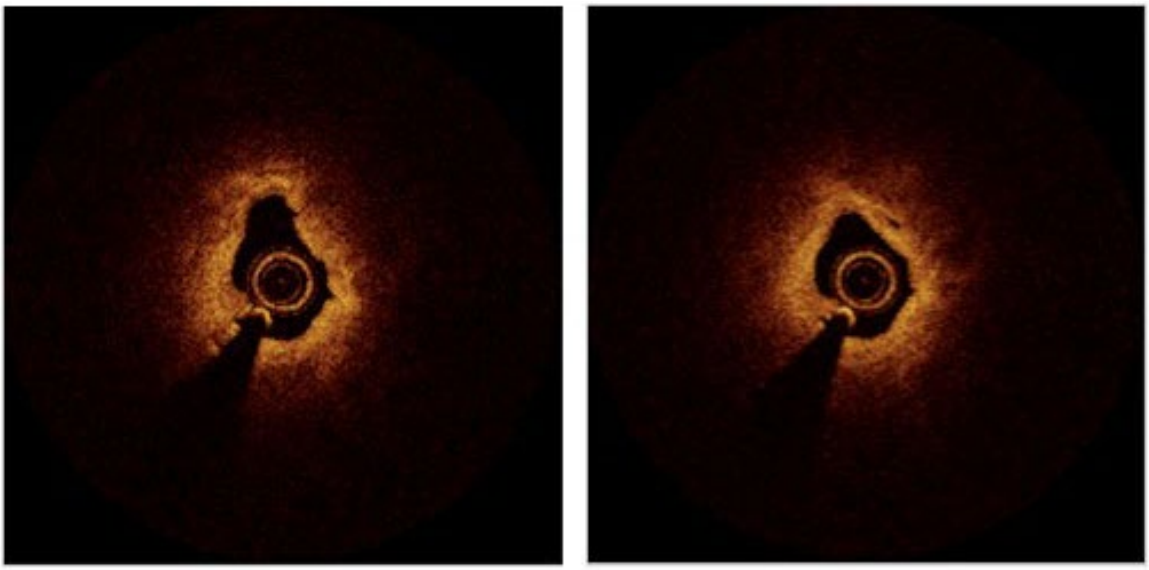

Figure 2. OCT images revealed plaque erosion was characterized by the presence of attached thrombus overlying an intact and visualized plaque

OCT image analysis

All OCT images were analyzed by the researcher and an experienced OCT investigator who was blinded to the clinical presentation and angiographic data. When there was disagreement between the investigators, a consensus reading was obtained.

OCT image features

The presence of fibrous cap disruption (PR, PE, CN, lipid plaque, fibrous plaque, calcified plaque, or intracoronary thrombus) was recorded. PR was identified by the presence of fibrous cap discontinuity and cavity formation in the plaque (Figure 1). PE was characterized by the presence of thrombus overlying an intact plaque (Figure 2). CN was defined as fibrous cap disruption over a calcified plaque, characterized by protruding calcification, superficial calcium deposition, and the presence of a substantial amount of calcium proximal and/or distal to the lesion (Figure 3) [7]. Culprit lesions

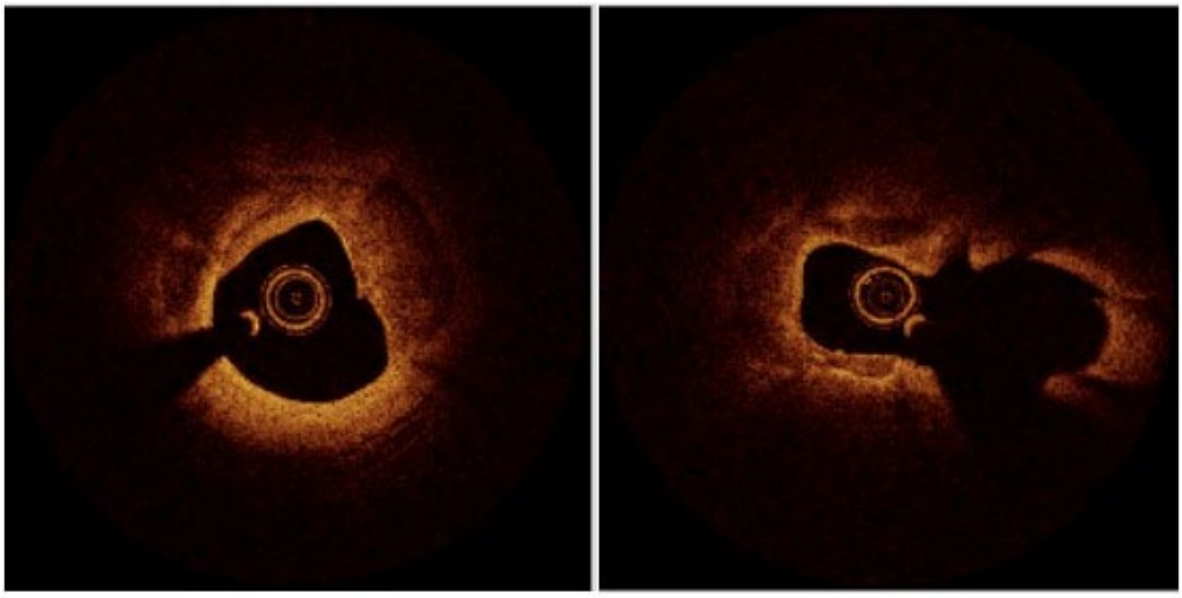

Figure 3. OCT demonstrateCalcified nodule was defined when fibrous cap disruption was detected over a calcidied plaque characterized by protruding calcification, superficial calcium, and the presence of substantive calcium proximal and/or distal to the lesion

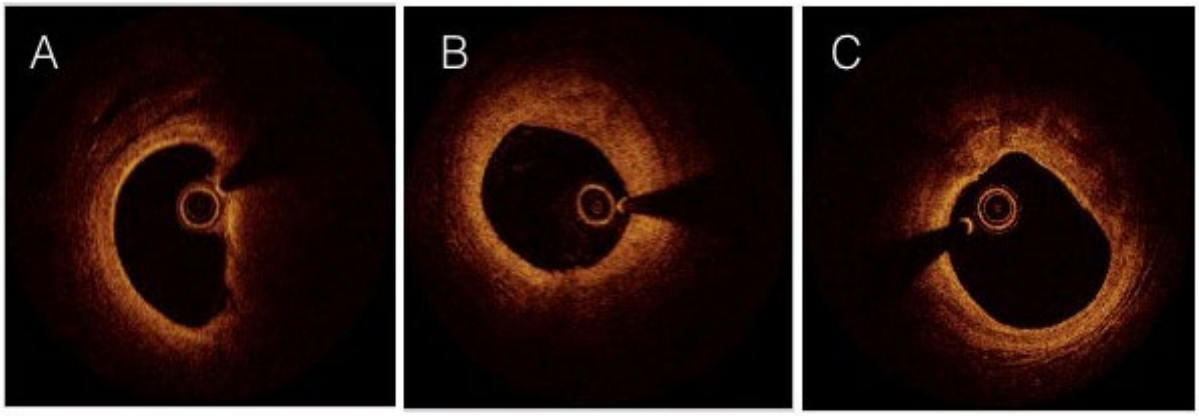

Figure 4. OCT revealed lipid plaques as signal-poor regions with diffuse borders(A). fibrous plaques were defined as homogeneous signal-rich regions(B), fibrocalcific plaques as signal poor regions with sharp borders(C).

that did not meet the criteria for PR, PE, or CN were classified as "other". Fibrous plaques were defined as homogeneous signal-rich regions, fibrocalcific plaques as signal-poor regions with clearly defined borders, and lipid plaques as signal-poor regions with diffuse borders (Figure 4). OCT is also capable of differentiating red and white thrombus. A red thrombus was defined as a protruding mass, characterized by high back-scattering with signal-free shadowing inside the vessel lumen, and white thrombus (platelet-rich) was defined as a lesion with low back-scattering [8] (Figure 5). Owing to its high resolution, OCT can also demonstrate thick-cap fibroatheroma (TCFA), defined as a plaque with a thin fibrous cap of ≤ 65 µm thickness.

Statistical analysis

Data are shown as mean ± SD. Comparisons between two groups were performed using Fisher's exact test. ANOVA or the Kruskal-Wallis test was used to compare data relating to PR, PE, and CN, and comparisons between two groups were made using the unpaired t-test or Mann-Whitney U test. $P < 0.05$ was accepted as indicating statistical significance.

Results

Baseline characteristics of the participants

A total of 22 patients with ACS were enrolled. The baseline characteristics of participants in whom PR, PE, CN, or other unspecified lesions were identified are summarized in Table 1. The mean age of the participants was 67 years and 64% of them were men. With respect to coronary risk factors, the prevalences of hypertension, diabetes, and smoking were 63.6%, 31.8%, and 40.9%, respectively. The prevalence of STEMI was 32%.

A comparison of the characteristics of participants with PR, PE, and CN is shown in Table 2. The participants with PR tended to be younger than those with the other two types of lesions (66 years old), but there were no significant differences in any of the characteristics of the three groups. However, the participants with CN were more likely to have CKD stage III and a high creatinine concentration than those with PR or PE.

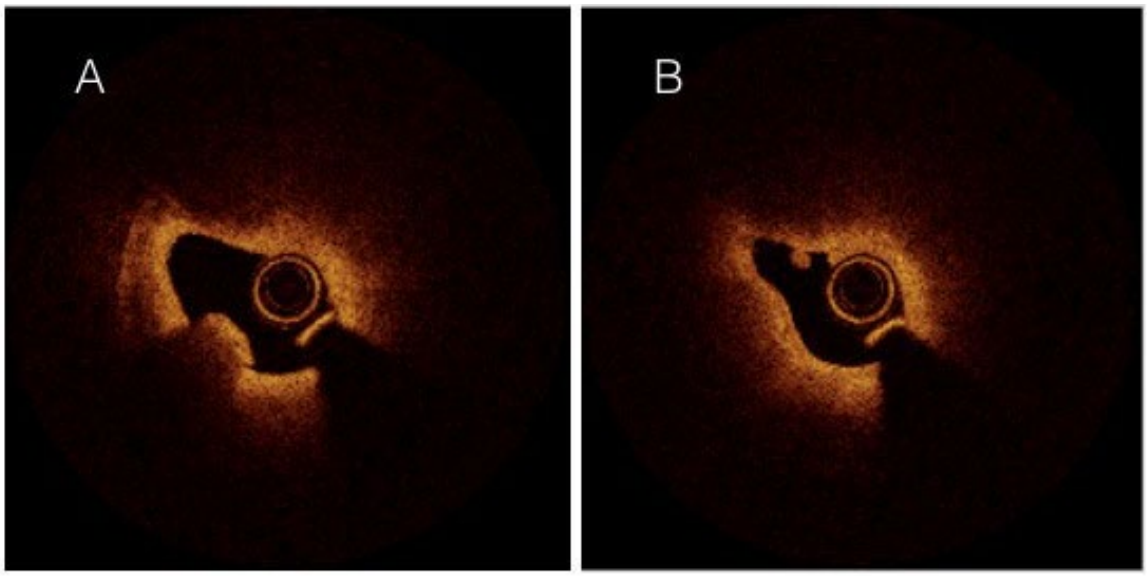

Figure 5. OCT demonstrated red thrombus were demonstrated as a high backscattering protrusion mass with signal-free shadowing inside the vessel lumen (A), and white thrombus (platelet-rich) were revealed as low-backscattering projection (B)

Table 1. Baseline characteristics of the participants

	Full cohort (n=22)	Classified (n=20)	Other (n=2)	*P*-value
Age	67.6 ± 9.6	67.8 ± 10.0	66.0 ± 4.2	0.812
Men	14 (63.6%)	13 (65.0%)	1 (50.0%)	1.000
Body mass	66.8 ± 7.6	66.7 ± 7.7	68.0 ± 9.9	0.694
Height	162.0 ±7.3	162.2 ± 6.9	160.0 ± 14.1	0.825
BMI	25.6 ± 3.4	25.4 ± 2.9	27.2 ± 8.6	0.815

Table 1. Baseline characteristics of the participants (Continue)

	Full cohort (n=22)	Classified (n=20)	Other (n=2)	*P*-value
Risk factors				
Hypertension	14 (63.6%)	13 (65.0%)	1 (50.0%)	1.000
Diabetes mellitus	7 (31.8%)	7 (35.0%)	0 (0.0%)	1.000
Dyslipidemia	14 (63.6%)	13 (65.0%)	1 (50.0%)	
Chronic kidney disease	15 (68.2%)	14 (70.0%)	1 (50.0%)	1.000
Chronic kidney disease (stage II)	10 (45.5%)	9 (45.0%)	1 (50.0%)	1.000
Chronic kidney disease (stage III)	5 (22.7%)	5 (25.0%)	0 (0.0%)	
Family history of CAD	4 (18.2%)	3 (15.0%)	1 (50.0%)	0.338
Smoking	9 (40.9%)	9 (45.0%)	0 (0.0%)	0.494
Alcohol	3 (13.6%)	3 (15.0%)	0 (0.0%)	1.000
Presentation				
NSTE-ACS	15 (68.2%)	14 (70.0%)	1 (50.0%)	1.000
STEMI	7 (31.8%)	6 (30.0%)	1 (50.0%)	

BMI= body mass index, CAD= coronary artery disease, NSTE-ACS= non-ST-segment elevation acute coronary syndrome, STEMI= ST-segment elevation myocardial infarction.

Incidence of plaque rupture, plaque erosion, and calcified nodule in the participants

Of the 22 culprit lesions identified, 16 (73%) were classified as PR, 2 (9%) were classified as plaque erosion, calcified nodule, and others (Figure 6).

Table 2. Baseline characteristics of the participants with plaque rupture, plaque erosion, or calcified nodule

	PR (n=16)	PE (n=2)	CN (n=2)	P-value	P-value		
					PR vs. PE	PE vs. CN	PR vs. CN
Age	65.7 ± 9.4	72.0 ± 9.9	80.0 ± 8.5	0.131	0.385	0.477	0.058
Men	10 (62.5%)	1 (50.0%)	2 (100.0%)	0.775			
Body mass (kg)	66.8 ± 7.5	72.0 ± 2.8	60.5 ±12.0	0.343	0.356	0.319	0.299
Height (cm)	162.3 ± 6.8	162.5 ± 10.6	161.5± 9.2	0.989	0.963	0.929	0.888
BMI	25.4 ± 3.0	27.4 ± 2.5	23.0 ± 2.0	0.349	0.395	0.195	0.293
Risk factors							
Hypertension	10 (62.5%)	2 (100.0%)	1 (50.0%)	0.775	0.529	1.000	1.000
Diabetes mellitus	5 (31.3%)	1 (50.0%)	1 (50.0%)	1.000	1.000	1.000	1.000
Dyslipidemia	11 (68.8%)	1 (50.0%)	1 (50.0%)	1.000	1.000	1.000	1.000
CKD stage III	3 (18.8%)	0 (0.0%)	2 (100.0%)	0.104	1.000	0.333	0.065
FH of CAD	3 (18.8%)	0 (0.0%)	0 (0.0%)	1.000	1.000	N/A	1.000
Smoking	7 (43.8%)	1 (50.0%)	1 (50.0%)	1.000	1.000	1.000	1.000
Alcohol	3 (18.8%)	0 (0.0%)	0 (0.0%)	1.000	1.000	N/A	1.000
Presentation							
NSTE-ACS	11 (68.7%)	1 (50.0%)	2 (100.0%)	1.000	1.000	1.000	1.000

Table 2. Baseline characteristics of the participants with plaque rupture, plaque erosion, or calcified nodule (Continue)

	PR (n=16)	PE (n=2)	CN (n=2)	P-value	P-value		
					PR vs. PE	PE vs. CN	PR vs. CN
STEMI	5 (31.3%)	1 (50.0%)	0 (0.0%)				
Laboratory parameters							
HCT, mg/dL	42.0 ± 4.8	39.4 ± 5.5	37.1 ± 7.6	0.388	0.479	0.763	0.209
Creatinine, mg/dL	1.0 ± 0.2	0.8 ± 0.5	1.2 ± 0.0	0.303	0.673	0.121	0.049
AST activity	56.2 ± 44.6	31.6 ± 10.5	27.1 ± N/A	N/A	0.399	N/A	N/A
ALT activity	43.1 ± 54.0	42.1 ± 4.7	15.8 ± N/A	N/A	0.399	N/A	N/A

PR = plaque rupture, PE = plaque erosion, CN = calcified nodule, FH = family history, CKD = chronic kidney disease, CAD = coronary artery disease, HCT = hematocrit, AST = aspartate aminotransferase, ALT = alanine aminotransferase.
PR = plaque rupture, PE = plaque erosion, CN = calcified nodule

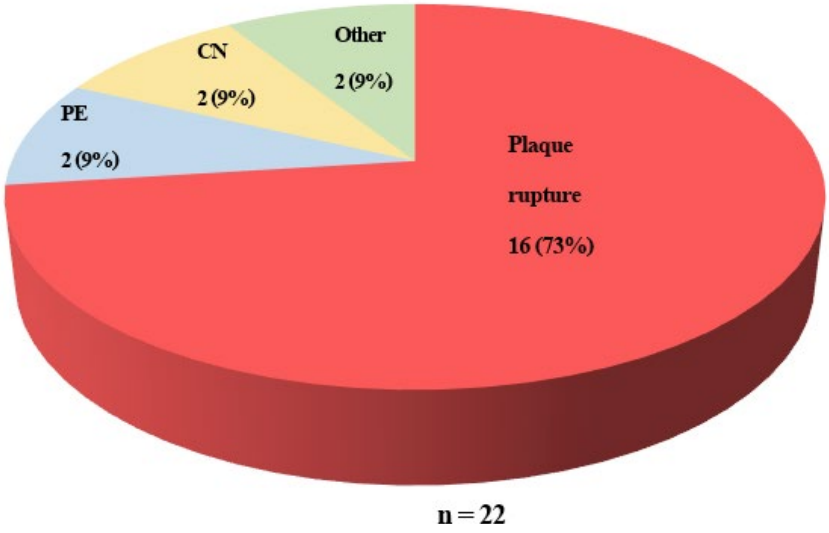

Figure 6. incidence of plaque rupture, plaque erosion, and calcified nodule

Angiographic findings

The lesion distribution is summarized in Table 3. PR was most prevalent in the LAD, followed by the RCA, and least prevalent in the LCX. All of the PE lesions were identified in the LAD, but CN lesions were equally prevalent in the LAD and RCA.

Characteristics of the plaques, determined using OCT

Thrombus was identified in all the PR lesions, and red thrombus was more prevalent than white thrombus. PR was present in 100% of the lipid plaques, 87.5% of calcified plaques, and 75% of the fibrous plaques; whereas PR and PE tended to be associated with fibrous plaque. There were no significant differences in the prevalence of TCFA among participants with the various lesions: it was present in 15 (93.8%), 2 (100%), and 1 (50%) of the participants with PR, PE, and CN, respectively. The mean MLD was higher in participants with CN (1.5 ± 0.5 mm) than in those with PE or CN (p = 0.047)

Table 3. Distribution of angiographic lesions

	PR	PE	CN	*P*-value	*P*-value		
					PR vs. PE	PE vs. CN	PR vs. CN
Lesion location							
LAD	12 (75.0%)	2 (100.0%)	1 (50.0%)	0.718	1.000	1.000	0.490
LCX	1 (6.2%)	0 (0.0%)	0 (0.0%)				
RCA	3 (18.8%)	0 (0.0%)	1 (50.0%)				

PR = plaque rupture, PE = plaque erosion, CN = calcified nodule.

Table 4. Plaque characteristics, identified using OCT

	PR (n=16)	PE (n=2)	CN (n=2)	*P*-value	*P*-value		
					PR *vs*. PE	PE *vs*. CN	PR *vs*. CN
Thrombus	16 (100.0%)	2 (100.0%)	1 (50.0%)	0.200	N/A	1.000	N/A
Red thrombus	14 (87.5%)	1 (50.0%)	1 (50.0%)	0.162	0.314	1.000	0.314
White thrombus	8 (50.0%)	1 (50.0%)	0 (0.0%)	0.728	1.000	1.000	0.477
Calcified plaque	14 (87.5%)	2 (100.0%)	2 (100.0%)	1.000	1.000	N/A	1.000
Lipid plaque	16 (100.0%)	2 (100.0%)	2 (100.0%)	N/A	N/A	N/A	N/A
Fibrous plaque	12 (75.0%)	2 (100.0%)	0 (0.0%)	0.155	1.000	0.333	0.098
TCFA< 0.065 µm	15 (93.8%)	2 (100.0%)	1 (50.0%)	0.126	0.261	0.221	0.083
TCFA	0.04 ± 0.02	0.05 ± 0.01	0.05 ± 0.06	0.731	0.370	1.000	0.883
MLA	1.5 ± 0.4	1.2 ± 0.1	2.4 ± 1.6	0.350	0.261	0.221	0.399
MLD	1.0 ± 0.2	1.0 ± 0.1	1.5 ± 0.5	0.047	0.791	0.2415	0.020
Length (mm)	32.8 ± 16.7	27.1 ± 8.8	11.0 ± 8.7	0.207	0.779	0.121	0.092
RVD	3.4 ± 0.5	2.8 ± 0.3	3.7 ± 0.2	0.139	0.097	0.060	0.399

PR = plaque rupture, PE = plaque erosion, CN = calcified nodule, TCFA = thin cap fibroatheroma, MLA = minimum luminal area, MLD = minimum luminal diameter, RVD = reference vessel diameter.

Discussion

This study represents the first systematic characterization of the pathophysiology of the three most common causes of ACS performed using OCT in Thailand. OCT provides higher resolution images of intravascular structures than IVUS. The principal findings were that OCT is an effective means of classifying the pathophysiology of ACS as PR, PE, or CN; and that it is also an ideal tool for the identification of microvascular structures, such as vulnerable plaque and TCFA, for the classification of the type of thrombus.

Prevalences of plaque rupture, plaque erosion, and calcified nodule in patients with ACS

The most common causes of acute thrombosis in patients with ACS are PR, PE, and CN [(1)]. Previous autopsy findings showed that thrombosis of the coronary artery resulted from PR in 60% of participants and from PE in 40% of participants [(9)]. In addition, Farb et al. studied 50 cases of sudden death owing to coronary thrombosis, and identified thin fibrous cap rupture in 28 patients and erosion in 22 patients [(10)]. Furthermore, Hisaki et al. [(11)] performed a histopathological study in patients with ACS who experienced sudden coronary death, and identified 70 PR lesions and 54 PE

lesions among the 122 postmortem lesions identified. In the present study, the prevalence of PR was 73%, which is similar to that previously reported, and that of PE was 9%, which is lower. The prevalence of CN, the least common pathology in patients with ACS, was 9% in the present study, which is not dissimilar to the previously reported prevalence of 4%–7% [12].

Characteristics of patients with plaque rupture, plaque erosion, or calcified nodule

A previous postmortem study of individuals who had experienced coronary sudden death revealed a significantly higher prevalence of PE in younger women, with a mean age of 44±7 years [10]. Burke et al. [13] demonstrated that PE is significantly associated with smoking, with approximately 78%. In the present study, we found that patients with PE were older than those with PE. Furthermore, 50% of those with PE were women, which implies a lower prevalence in this sex than that identified in the previous study. This disparity may be the result of differing characteristics of the participants. Recent studies have shown that coronary calcification is more prevalent in patients with CKD than in those with normal kidney function [14–15]. We also found that participants with CN had higher circulating creatinine concentrations and tended to have a higher prevalence of CKD stage III than those with PN or PE. Finally, PR was more common in men, which is compatible with the present data.

Plaque characteristics, identified using OCT

We found that lipid plaques were the only ones to undergo PR. In addition, fibrous plaque was present in 100% and 75% of participants with PE or PR, respectively. Fibrin-rich red thrombi predominated in participants with PR (87.5%), whereas white thrombus was found in approximately 50% of participants with PE or CN. The mean MLD was highest in participants with CN (p=0.047).

Clinical implications

The distinct characteristics of the pathophysiology of patients with ACS, reflected in the differing lesions of PE, PR, and CN, imply differing causes and the necessity for differing treatments. PE has previously been shown to be associated with less thrombus than PR [16], and this may imply that less invasive treatments, such as medication without stent implantation, may be possible. However, further studies should be conducted to investigate this possibility.

Limitations

The present study had several limitations. First, the discrepancy between our data and those obtained in previous studies might be the result of differences in the participants and in the size of the studies. Second, the presence of thrombus overlying culprit lesions might have obscured the pathology and plaque characteristics. Third, we permitted the use of small balloons (smaller than the reference vessel diameter) for pre-dilatation in cases of STEMI or critical lesions, to avoid contamination with blood during pullback, causing back-scattering and poor images, which may have affected the features of the culprit lesion that were identified.

Conclusion

In the present study, we found that OCT represents an excellent intracoronary imaging modality for the characterization of the pathophysiology of ACS, in the forms of PR, PE, and CN. PR is the most common pathology in patients with ACS, accounting for 73% of the lesions in the present study. PE tended to be associated with the lowest MLA of the three pathologies and CN was commoner in older patients. In addition, CN was associated with higher creatinine concentrations and MLD than PR.

Acknowledgments

We thank Mark Cleasby, PhD from Edanz (www.edanz.com/ac) for editing a draft of this manuscript.

References

1. Virmani R, Burke AP, Farb A, Kolodgie FD. Pathology of the vulnerable plaque. *J Am Coll Cardiol*. 2006;47(8 Suppl):C13–C18.
2. Naghavi M, Libby P, Falk E, Casscells SW, Litovsky S, Rumberger J, et al. From Vulnerable Plaque to Vulnerable Patient: A Call for New Definitions and Risk Assessment Strategies: Part I. *Circulation*. 2003;108:1664–1672.
3. Abtahian F, Jang I-K. Optical Coherence Tomography. *In Braunwald's Heart Disease*, 10th edition, volume 1. 2015;276–289.
4. Kubo T, Imanishi T, Takarada S, Kuroi A, Ueno S, Yamano T, et al. Assessment of culprit lesion morphology in acute myocardial infarction: ability of optical coherence tomography compared with intravascular ultrasound and coronary angioscopy. *J Am Coll Cardiol*. 2007;50:933–939.
5. Jang I-K, Bouma BE, Kang D-H, Park S-J, Park S-W, Seung K-B, et al. Visualization of coronary atherosclerotic plaques in patients using optical coherence tomography: comparison with intravascular ultrasound. *J Am Coll Cardiol*. 2002;39:604–609.
6. Yabushita H, Bouma BE, Houser SL, Aretz HT, Jang I-K, Schlendorf KH, et al. Characterization of Human Atherosclerosis by Optical Coherence Tomography. *Circulation*. 2002;106:1640–1645.
7. Jia H, Abtahian F, Aguirre AD, Lee S, Chia S, Lowe H, et al. In Vivo Diagnosis of Plaque Erosion and Calcified Nodule in Patients With Acute Coronary Syndrome by Intravascular Optical Coherence Tomography. *J Am Coll Cardiol*. 2013;62:1748–1758.
8. Akasaka T, Kubo T, Mizukoshi M, Tanaka A, Kitabata H, Tanimoto T, et al. Pathophysiology of acute coronary syndrome assessed by optical coherence tomography. *J Cardiol.* 2010;56:8–14.
9. van der Wal AC, Becker AE, van der Loos CM, Das PK. Site of intimal rupture or erosion of thrombosed coronary atherosclerotic plaques is characterized by an inflammatory process irrespective of the dominant plaque morphology. *Circulation*. 1994;89:36–44.
10. Farb A, Burke AP, Tang AL, Liang TY, Mannan P, Smialek J, et al. Coronary plaque erosion without rupture into a lipid core. A frequent cause of coronary thrombosis in sudden coronary death. *Circulation*. 1996;93:1354–1363.
11. Hisaki R, Yutani C. Plaque Morphology of Acute Coronary Syndrome. *J Atheroscler Thromb*. 1998;4:156–161.
12. Virmani R, Kolodgie FD, Burke AP, Farb A, Schwartz SM. Lessons from Sudden Coronary Death: A Comprehensive Morphological Classification Scheme for Atherosclerotic Lesions. *Arterioscler Thromb Vasc Biol*. 2000;20:1262–1275.
13. Burke AP, Farb A, Malcom GT, Liang Y, Smialek J, Virmani R. Effect of risk factors on the mechanism of acute thrombosis and sudden coronary death in women. *Circulation*. 1998;97:2110–2116.
14. Budoff MJ, Rader DJ, Reilly MP, Mohler ER, Lash J, Yang W, et al. Relationship of Estimated GFR and Coronary Artery Calcification in the CRIC (Chronic Renal Insufficiency Cohort) Study. *Am J Kid Dis*. 2011;58:519–526.
15. Koukoulaki M, Papachristou E, Kalogeropoulou C, Papathanasiou M, Zampakis P, Vardoulaki M, et al. Increased Prevalence and Severity of Coronary Artery Calcification in Patients with Chronic Kidney Disease Stage III and IV. *Nephron Extra*. 2012;2:192–204.
16. Kramer MCA, Rittersma SZH, de Winter RJ, Ladich ER, Fowler DR, Liang Y-H, et al. Relationship of Thrombus Healing to Underlying Plaque Morphology in Sudden Coronary Death. *1J Am Coll Cardiol*. 2010;55:122–32.

License, Supplymentary Material and Copyright

This is an open-access article distribute under the terms of the Creative Commons Attribution (CC by NC ND 4.0) License. You may share the material, but must give appropriate credit to the source, provide a link to the license and indicate if changes were mades. You may not use the material for commercial purpose. If you remix, tranform, or build upon the material, you may not distribute the modified material

Any supplymentary material reference in the article can be found in the online version.

This article is copyright of the Chulabhorn Royal Academy, 2022

Citation

Viroj M, Plasat L, Chompol P, Sopon S, Tanyarat A, Supawat R, Nakarin S. Pathology of acute coronary syndrome, assessed using optical coherence tomography. *J Chulabhorn Royal Acad*. 2022; 4(2): 59-69. https://he02.tci-thaijo.org/index.php/jcra/article/view/253294

Online Access

https://he02.tci-thaijo.org/index.php/jcra/article/view/253294